Ecosystems (2005) 8: 760–778
DOI: 10.1007/s10021-005-0079-5

ECOSYSTEMS

Net Primary Production and Canopy Nitrogen in a Temperate Forest Landscape: An Analysis Using Imaging Spectroscopy, Modeling and Field Data

Scott V. Ollinger,[1]* and Marie-Louise Smith[2]

[1]*Complex Systems Research Center, Institute for the Study of Earth, Oceans and Space, University of New Hampshire, Durham, New Hampshire 03820, USA;* [2]*USDA Forest Service, Northeastern Research Station, P.O. Box 640 Durham, New Hampshire 03824, USA*

Abstract

Understanding spatial patterns of net primary production (NPP) is central to the study of terrestrial ecosystems, but efforts are frequently hampered by a lack of spatial information regarding factors such as nitrogen availability and site history. Here, we examined the degree to which canopy nitrogen can serve as an indicator of patterns of NPP at the Bartlett Experimental Forest in New Hampshire by linking canopy nitrogen estimates from two high spectral resolution remote sensing instruments with field measurements and an ecosystem model. Predicted NPP across the study area ranged from less than 700 g m^{-2} $year^{-1}$ to greater than 1300 g m^{-2} $year^{-1}$ with a mean of 951 g m^{-2} $year^{-1}$. Spatial patterns corresponded with elevation, species composition and historical forest management, all of which were reflected in patterns of canopy nitrogen. The relationship between production and elevation was nonlinear, with an increase from low- to mid-elevation deciduous stands, followed by a decline in upper-elevation areas dominated by evergreens. This pattern was also evident in field measurements and mirrored an elevational trend in foliar *N* concentrations. The increase in production from low-to mid-elevation deciduous stands runs counter to the generally accepted pattern for the northeastern U.S. region, and suggests an importance of moisture limitations in lower-elevation forests.

Field measurements of foliar N, wood production and leaf litterfall were also used to evaluate sources of error in model estimates and to determine how predictions are affected by different methods of acquiring foliar N input data. The accuracy of predictions generated from remotely sensed foliar N approached that of predictions driven by field-measured foliar N. Predictions based on the more common approach of using aggregated foliar N for individual cover types showed reasonable agreement in terms of the overall mean, but were in poor agreement on a plot-by-plot basis. Collectively, these results suggest that variation in foliar N exerts an important control on landscape-level spatial patterns and can serve as an integrator of other underlying factors that influence forest growth rates.

Key words: NPP; forest productivity; foliar nitrogen; carbon; hyperspectral remote sensing; AVIRIS; Hyperion; White Mountains; New Hampshire; elevation gradients; ecosystem model.

Received 16 May 2003; accepted 17 June 2004; published online 21 October 2005.
Corresponding author; e-mail: scott.ollinger@unh.edu

Introduction

The ability to detect, interpret and predict patterns of spatial heterogeneity in ecosystem function is a central and long-standing goal of ecology. This interest stems from the fact that spatial patterning often reflects variation in fundamental ecological processes and from the wide range of consequences that spatial heterogeneity can have on ecological, environmental and even economic factors (for example, Pickett and Cadenasso 1995; Burke and others 1997; Turner and others 2001). In temperate forests, interest in patterns of net primary productivity (NPP) has been fueled by the role forests play in the earth's carbon cycle. For example, recent estimates drawn from atmospheric models and field-based inventories suggest that temperate forests represent a carbon sink of between 0.5 and 2 Pg C $year^{-1}$ (Fan and others 1998; Houghton and others 1999; Bousquet and others 2000), or approximately 10 to 35% of the global carbon emissions from fossil fuel combustion (Schimel and others 1995). At present, large uncertainties exist in both the magnitude and spatial distribution of this sink, as well as the underlying mechanisms responsible.

Interestingly, whereas global-scale associations between NPP and broad climatic gradients have been understood for some time (for example, see Leith 1975), capturing landscape to regional-scale patterns has proven to be more challenging. At these scales, the influence of climate is often confounded by other sources of variation stemming from factors that can be difficult to characterize spatially. Examples include soil properties such as texture, mineralogy and nutrient supply (Pastor and others 1984; Cole 1995; Reich and others 1997), historical disturbance and human land use (for example, Motzkin and others 1999; Reed and others 1999), and biotic attributes such as herbivory, species composition and stand age (Gower and others 1996; Craine and others 2003).

In recent years, a growing number of studies have attempted to address this challenge through the coupled application of remote sensing and ecosystem simulation models (for example, He and others 1998; Ollinger and others 1998; Fournier and others 2000; Kimball and others 2000). Whereas remote sensing instruments collect spatially-continuous information on vegetation reflectance properties, models focus on the ecological processes that regulate assimilation and cycling of carbon, water and nutrients. Despite the benefits of this approach, the lack of detailed data for important rate-limiting variables, especially those related to nitrogen availability, represents a continuing hurdle (for example, Reich and others 1999a; Coops and Waring 2001).

Although spatially-explicit data for soil N status are rare, a growing body of research has demonstrated that canopy N concentrations can be estimated using high spectral resolution remote sensing, or imaging spectroscopy (Yoder and Pettigrew-Crosby 1995; Zagolski and others 1996; Martin and Aber 1997; Boegh and others 2002). Imaging spectroscopy differs from more conventional forms of remote sensing in that the full spectrum of reflected light is captured in a series of narrow optical bands, allowing more detailed analysis of vegetation reflectance features than is possible with broad-band sensors. The potential use of canopy nitrogen as an indicator of ecosystem spatial patterns stems from relationships between foliar N concentrations and maximum net photosynthesis (Field and Mooney 1986; Reich and others 1995, 1999b) and from linkages among foliar N, N cycling and growth (Pastor and others 1984; Wessman and others 1988; Smith and others 2002; Ollinger and others 2002). Integration of this approach with ecosystem modeling would bring several added benefits, among which are the opportunity to evaluate the accuracy of global NPP estimates, such as those generated from NASA's moderate resolution imaging spectrometer (MODIS, Running and others 2000) and the ability to examine how patterns of forest production relate to other landscape features, such as topography, forest composition and disturbance history.

In this study, we examined spatial patterns of forest productivity over a structurally and floristically diverse 25^2 km landscape centered around the Bartlett Experimental Forest (BEF) in central New Hampshire, USA. Our approach involved integration of a forest process model (PnET-II, Aber and others 1995) with spatially-explicit canopy nitrogen estimates, derived using both airborne and spaceborne imaging spectroscopy. We also used data for wood and leaf production collected from a network of measurement plots to validate model predictions and to help interpret relationships between predicted growth and landscape features such as elevation. Finally, to evaluate the degree to which remotely-sensed canopy nitrogen enhances our ability to determine NPP spatial patterns, we conducted several additional model analyses using alternative sources of foliar N input data; first using species-specific field measurements and then using mean values applied to broad cover type classifications.

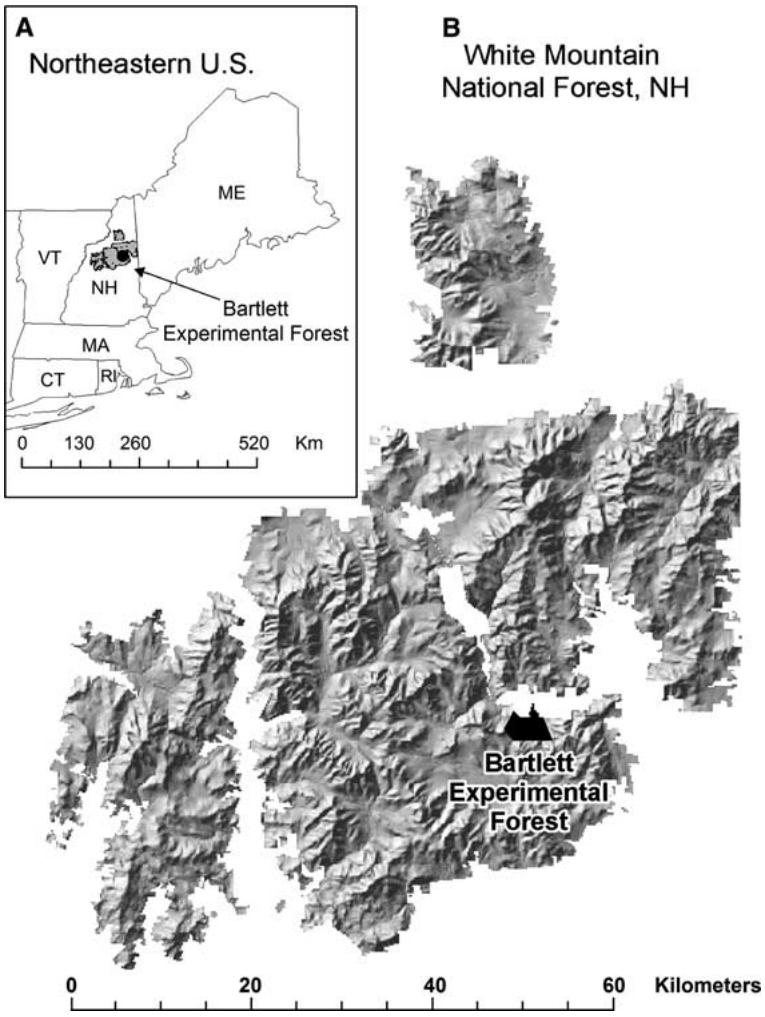

Figure 1. Location of the Bartlett Experimental Forest within the White Mountain National Forest in New Hampshire, USA. The *inset* shows the greater northeastern USA region.

Methods

Study Area

BEF (N 44.05, W 71.29) is located within the White Mountain National Forest, a heavily forested, mountainous region in north central New Hampshire, USA (Figure 1). Due to its broad elevational range (200–1,500 m), the region contains a wide variety of vegetation and site types, typical of those distributed across the northeastern U.S. These include mixed pine and oak forest types in valley bottoms, northern hardwood and mixed conifer forests on mid-slopes, spruce-fir forests on shallow bedrock and upper mountain slopes, and alpine tundra mountain tops. Soils are mostly coarse-textured spodosols or inceptisols formed on glacially-deposited tills.

Established in 1932 as a USDA Forest Service research forest, BEF is a 1,050 ha tract of secondary successional deciduous and coniferous forest located in the central portion of the White Mountains. It is representative of the larger White Mountain region, having similar vegetation composition, soil types, disturbance histories and topography, although the maximum elevation is somewhat lower at approximately 850 m.

In 1932 a network of permanent forest inventory plots (approximately 0.1 ha) were established on a regular grid, spaced 200 m by 100 m apart. All trees on a majority of these plots have been measured by 1-inch diameter classes in at least three time periods, the most recent complete re-measurement at the time of this study being in 1991–1992. All plots within BEF are believed to have a history of logging, although roughly 45% of the land area has remained uncut since at least 1890. The remaining areas have been subjected to a variety of harvesting practices. Some areas were also affected by a late 19th century fire and severe wind disturbance resulting from hurricanes in 1938 and 1954.

Productivity Measurements

In a related study, Smith and others (2002) sampled 56 0.1 ha plots across the White Mountains for foliar N concentrations and aboveground productivity. Here, we use data from a subset of those plots (n = 39) located at BEF. Plot elevations ranged from 220 to 731 m and represent a range in species composition and successional status. Major tree species include sugar maple (*Acer saccharum*), American beech (*Fagus grandifolia*), white ash (*Fraxinus Americana*), paper birch (*Betula papyrifera*), yellow birch (*Betula alleghaniensis*), red maple (*Acer rubrum*), pin cherry (*Prunus pennsylvanica*), eastern hemlock (*Tsuga canadensis*), red spruce (*Picea rubens*), balsam fir (*Abies balsamea*) and eastern white pine (*Pinus strobus*). Most plots contained mixtures of two or more species.

Above ground net primary productivity (ANPP, g m^{-2} $year^{-1}$) was estimated as the sum of wood production plus foliar production. Wood biomass (g m^{-2}) was estimated on all plots by measurement of stem diameter for all trees greater than 5 cm DBH, and converted to biomass using locally-derived allometric equations (Hocker and Early 1983; Tritton and Hornbeck 1981). Plot-level values were calculated by summing individual tree values over the entire plot and dividing by the plot area. Plot-level wood production (g m^{-2} $year^{-1}$) was calculated using the difference between woody biomass in a 1998 measurement campaign and a previous inventory (1991–1992) carrying forward the biomass of trees that died during the intervening years.

Foliar production was estimated on a subset of 15 plots using leaf litterfall collections. Eight litter collectors (0.23 m^2) were randomly placed in the selected plots during the late summer. Litter was collected every 2–3 weeks in the fall, once in the spring, and once at the end of the following summer. Litter from each collector was air dried and sorted into leaf and non-leaf litter. Leaf litter was sorted by species and then oven-dried at 70°C for 48 h and weighed. Annual foliar production (g m^{-2} $year^{-1}$) was calculated as the sum of foliar litterfall mass divided by litter collector area. On several occasions, litter collections produced fewer than eight samples due to baskets having been tipped over or damaged by bears. This had a minor effect on the total number of samples obtained, but to avoid introducing a bias, disturbed collections were not used in calculating plot-level averages. Additional detail for forest productivity measurement methods are provided by Smith and others (2002).

Leaf- and Canopy-level Chemistry Measurements

To determine growing season canopy chemistry at each plot, all dominant and co-dominant species were identified, and between two and five trees per species were selected for green leaf collection. Leaves were collected from several heights in the canopy using 12-gauge shotguns. Mid-summer green leaf samples were collected on each study plot in August, 1997 to coincide with the peak of the growing season and with an overflight by NASA's airborne visible/infrared imaging spectrometer (AVIRIS). An additional collection was made on a subset of 19 plots in August, 2000 for use with imagery from NASA's satellite-based Hyperion instrument, although cloud-free Hyperion data were not successfully acquired until August of 2001 (described in the following section). Although synchronous collection of field and image data would have been ideal, between-year differences in leaf nitrogen at BEF are typically small with respect to the much wider degree of spatial variation that occurs over the landscape (Smith and others 2003). Differences that occur over the course of a growing season can represent another potential source of bias, but this was not an issue given that field and image data were both collected in late August.

A benchtop visible and near infrared spectrophotometer (NIRSystems 6500) was used to determine leaf-level foliar N concentrations of oven-dried, ground foliage according to methods described by Bolster and others (1996). Because mass-based N concentration has been shown not to vary significantly in relation to vertical canopy gradients (Ellsworth and Reich 1993; O'Neill and others 2002), plot-level whole canopy nitrogen concentration (g N per 100 g foliar biomass) was calculated as the mean of foliar N concentrations for individual species in each stand, weighted by the fraction of canopy foliar mass per species (Smith and Martin 2001).

Collection and Analysis of Remote Sensing Data

Hyperspectral remote sensing, or imaging spectroscopy, is a form of optical remote sensing in which surface reflectance is examined in narrow and contiguous spectral regions that allow analysis of specific absorption features on a pixel by pixel basis. This type of information can be useful for ecological research because vegetation reflectance

measured by imaging spectrometers is the product of canopy biochemical constituents (for example, chlorophyll, nitrogen, lignin and cellulose) in conjunction with leaf and canopy structure (Asner 1998). A growing number of studies have demonstrated that hyperspectral data from both airborne and spaceborne platforms can be used to estimate forest canopy chemistry (Wessman and others 1988; Zagolski and others 1996; Curran and others 1997; Martin and Aber 1997; Townsend and others 2003), and to identify vegetation types and species composition (Martin and others 1998; Roberts and others 1998; Kokaly and others 2003).

For this study hyperspectral remote sensing scenes were obtained for BEF from NASA's AVIRIS and Hyperion sensors. The AVIRIS instrument measures reflected solar radiance in 224 contiguous optical bands from 0.4 to 2.4 μm with a spectral resolution of 0.01 μm (Green and others 1998). AVIRIS was flown on an ER-2 aircraft at an altitude of 20,000 m, producing a spatial resolution of 17 m. Data for BEF and surrounding areas were collected on 12 August 1997, under nearly cloud-free conditions. AVIRIS data were converted from radiance (in units of $\mu W\ cm^{-2}\ nm^{-1}\ sr^{-1}$) to surface reflectance using the atmosphere removal program (ATREM; Gao and others 1993), which was designed specifically for removal of atmospheric absorption features from AVIRIS data. AVIRIS data were geometrically registered to within 0.5 pixel accuracy using a registered image from the SPOT satellite.

The Hyperion instrument is part of NASA's Earth Observing-1 (EO-1) satellite, which was launched in November, 2000. EO-1 orbits the earth at an altitude of 705 km and flies in close formation with the Landsat-7 satellite. Hyperion's detection capabilities are similar to those of AVIRIS (220 spectral bands ranging from 0.4 to 2.5 μm, with a 0.01 μm spectral resolution), but with a spatial resolution of 30 m. The swath width is 7.5 km and data are typically collected in 7.5 km by 100 km images. EO-1 was intended primarily to test new engineering capabilities, with scientific applications a secondary goal. As a consequence, Hyperion has a lower signal-to-noise ratio than AVIRIS. The signal-to-noise ratio of AVIRIS is greater than 600:1 over most of its spectral range (Green and others 1999), while Hyperion's signal-to-noise ratio does not exceed 200:1 (Barry 2001). In this study, use of Hyperion data alongside data from AVIRIS was intended to examine the degree to which these differences would affect its usefulness in applications of canopy biochemistry and productivity modeling.

A Hyperion scene for BEF and surrounding areas was acquired on August 29, 2001. Data were transformed from units of radiance ($\mu W\ cm^{-2}\ nm^{-1}\ sr^{-1}$) to surface reflectance using the ACORN atmospheric correction program (Analytical Imaging and Geophysics 2002). The use of different atmospheric correction programs for AVIRIS and Hyperion may produce some difference in the resulting reflectance estimates, although we expect this effect to be small relative to those arising from between-year atmospheric differences and differences due to sensor design. The Hyperion image was geometrically registered using the geo-registered AVIRIS image. Detailed information on Hyperion specifications and data pre-processing methods are reported elsewhere (Barry 2001; Jupp and others 2002; Ungar and others 2003).

Methods for deriving canopy N coverages from AVIRIS and Hyperion are given in Smith and others (2002, 2003) and can be summarized as follows. For both instruments, reflectance spectra for pixels covering each plot were used for comparison with field measured foliar nitrogen. Prior to calibration, reflectance values (R) were converted to absorbance (A) using the equation $A = \log_{10}(1/R)$, and a derivative transformation was applied. The derivative spectrum provides a measure of the slope of the reflectance curve at every point and results in a spectrum in which baseline offsets (caused, for example, by varying sun-earth-sensor geometry) have been removed or substantially minimized (Hruschka 1987). Two regions associated with water absorption (centered near 1.45 and 1.90 μm) were excluded from the analysis. AVIRIS and Hyperion wavelengths below 0.45 μm and HYPERION wavelengths above 2.0 μm were also excluded due to low signal-to-noise.

Relationships between plot-level spectra and canopy nitrogen were examined using partial least squares (PLS) regression, in which the full reflectance spectrum is collapsed into a smaller set of independent variables, or factors, with the measured canopy N data used directly during the spectral decomposition process (Kramer 1998). The accuracy of the resulting regression models was evaluated using an iterative cross-validation procedure in which each plot is sequentially excluded from the analysis and a canopy N prediction is generated from the remaining samples. All prediction residuals were then combined to compute validation statistics and residual mean square error of prediction (RMSEP). The RMSEP is the average prediction error expressed in units of N concentration (g N 100 g^{-1} dry matter) and is effectively

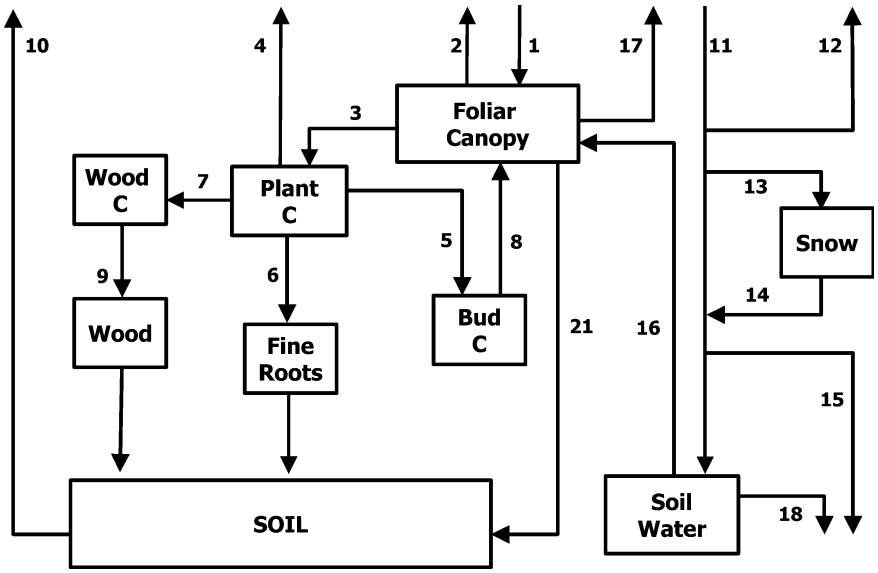

Figure 2. Structure of PnET-II. *Boxes* represent pools and numbered arrows represent fluxes: *1* Gross photosynthesis, *2* Foliar respiration, *3* Transfer to mobile C, *4* Growth and maintenance respiration, *5* Allocation to buds, *6* Allocation to fine roots, *7* Allocation to wood, *8* Foliar production, *9* Wood production, *10* Soil respiration, *11* Precipitation, *12* Canopy interception & evaporation, *13* Snow-rain partitioning, *14* Snowmelt, *15* Macro-pore flow, *16* Plant uptake, *17* Transpiration, *18* H_2O drainage.

equivalent to the standard error of prediction (SEP) for an independent data set (Kramer 1998).

Ecosystem Modeling

Model Description

PnET-II (Figure 2, Aber and others 1995) is a monthly time step, canopy- to stand-level model, initially developed in the northeastern U.S. and validated in a number of temperate forest systems, in which the productive potential of forest canopies is dependent on the relationship between photosynthetic capacity and canopy nitrogen (Field and Mooney 1986; Reich and others 1999b) and on the scaling of leaf structure and function through the canopy (Aber and others 1996). Stomatal conductance varies with photosynthesis such that water use efficiency is a function of CO_2 gain and is inversely related to atmospheric vapor pressure deficit. Hence, transpiration becomes a function of both canopy photosynthesis and climate, providing a dynamic link between fluxes of carbon and water.

These relationships are used to construct a multilayered forest canopy in which available light and leaf mass per unit area (LMA) decline with canopy depth. Light is attenuated through the canopy according to the Beer-Lambert exponential decay equation ($y = e^{-k*LAI}$). Changes in LMA are based on Ellsworth and Reich (1993) producing canopy gradients in area-based, but not mass-based foliar N concentration. Photosynthesis is calculated in a numerical integration over 50 canopy layers to capture the effect of gradual light extinction on total canopy carbon gain. Photosynthetic response curves for light and temperature were derived by Aber and Federer (1992). The photosynthetic response to vapor pressure deficit (VPD) is determined as a power function and actual evapotranspiration and moisture stress are calculated as functions of plant water demand and available soil water.

Model Application

PnET-II requires a number of input parameters summarizing vegetation and site characteristics (Table 1), along with monthly climatic data. Vegetation parameters include foliar N, LMA, leaf retention time and growing-degree day variables describing the phenology of leaf production and senescence. Required climatic and environmental inputs include temperature, precipitation, photosynthetically-active radiation (PAR), and soil water holding capacity (WHC).

For pixel-by-pixel application at BEF, PnET-II was run in conjunction with image-derived foliar N estimates and a 20 m resolution digital elevation model (DEM). For each pixel, geographic coordinates and elevation were extracted and used to estimate maximum and minimum temperature, vapor pressure, precipitation and PAR (30 year mean, Ollinger and others 1995). Although qualitative soil descriptions at BEF were available from Leak (1982), mapped estimates of WHC were not. Instead, we used the value of 120 mm calculated for the nearby Hubbard Brook Experimental Forest by Federer (1982).

Canopy Traits for Deciduous, Evergreen and Mixed Stands

A challenge encountered when using remotely-sensed vegetation variables in ecosystem modeling

Table 1. Input Parameters Required for Model Simulations and Values Used

Parameter	Description	Value	
		Decid.	Evergreen
Site variables			
Lat	Latitude	44.05	44.05
WHC	Soil water holding capacity (cm)	12	12
Canopy variables			
k	Canopy light attenuation constant	0.58	0.5
FolNCon	Foliar nitrogen (% by mass)	varies	Varies
FolReten	Foliage retention time (years)	1	3
SLWMax	Top canopy specific leaf weight (g m^{-2})	100	170
SLWDel	Change in SLW with increasing foliar mass above (g m^{-2} g^{-1})	0.2	0
FolRelGroMax	Maximum relative growth rate for foliage (y^{-1})	0.95	0.3
GDDFolStart	Growing degree days of foliage production onset	100	300
GDDFolEnd	Growing degree days of at which foliage production ends	900	1400
GDDWoodStart	Growing degree days of wood production onset	100	300
GDDWoodEnd	Growing degree days of at which wood production ends	900	1400
Photosynthesis variables			
AmaxA	Intercept { For relationship between Foliar N and max	−0.46	5.3
AmaxB	Slope { photosynthesis (mmol CO_2 m^{-2} leaf s^{-1} }	71.5	21.5
BaseFolRespFrac	Respiration as a fraction of max. photosynthesis	0.1	0.1
HalfSat	Half saturation light level (mmol m^{-2} s^{-1})	200	200
AmaxFrac	Daily Amax as a fraction of early morning instantaneous rate	0.75	0.75
PsnTOpt	Optimum temperature for photosynthesis °C	24	20
PSNTMin	Minimum temperature for photosynthesis °C	4	0
RespQ10	Q10 value for respiration	2	2
Water balance variables			
DVPD1	{ coefficients for power function converting	0.05	0.05
DVPD2	{ VPD to fractional loss in photosynthesis }	2	2
PrecIntFrac	Fraction of precipitation intercepted and evaporated	0.11	0.15
WUEConst	Constant in equation for WUE as a function of VPD	10.9	10.9
FastFlowFrac	Fraction of water inputs lost directly to drainage	0.1	0.1
f	Soil water release parameter	0.04	0.04
Carbon allocation variables			
CFracBiomass	Carbon fraction of biomass	0.45	0.45
RootAllocA	Intercept { For relationship between	0	0
RootAllocB	Slope { foliar and root allocation }	2	2
GRespFrac	Growth respiration, as a fraction of allocation	0.25	0.25
RootMRespFrac	Ratio of fine root maintenance respiration to biomass production	1	1
WoodMRespA	Wood maintenance respiration as a fraction of photosynthesis	0.07	0.07
PlantCReserveFrac	Fraction of PlantC held in resent after allocation to bud carbon	0.75	0.75
MinWoodFolRatio	Minimum ratio of carbon allocation to wood and foliage	1.5	1.25

is the problem of how to treat mixed pixels (those containing more than one functional group). In the present study, this was an important issue because PnET-II uses different foliar *N*–Amax relationships for deciduous and evergreen canopies, whereas image data provide only a single foliar N estimate based on the aggregated reflectance recorded for each pixel. For mixed pixels, the result is that remotely-derived foliar N values should fall somewhere between the actual values for each functional group, producing an underestimation for deciduous forests and an overestimation for evergreen forests. Although we might expect these errors to compensate for one another, differences in the slopes of the Amax–foliar N equations contained in the model make more explicit treatment necessary.

We dealt with this issue using an empirical approach that allowed partitioning of image-derived % N estimates into the relative proportions of

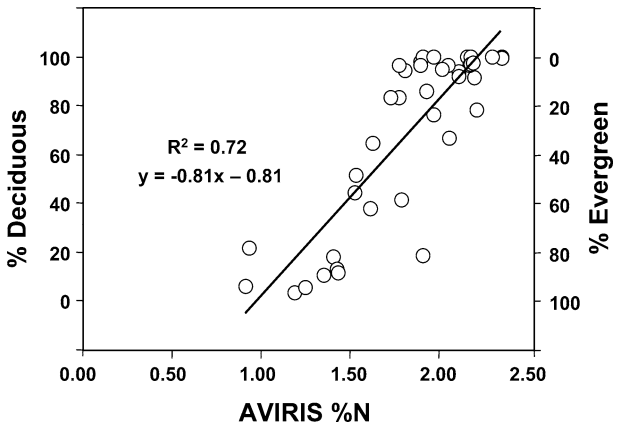

Figure 3. Forest composition as a fraction of deciduous and evergreen species on 0.1 ha field plots in relation to the plot-level canopy *N* concentration (percent by leaf mass), as estimated using AVIRIS. Proportions were based on relative canopy mass estimates, obtained using vertical canopy profiles.

deciduous and evergreen forests and the foliar N concentration of each component. This method was based on significant linear relationships observed among remotely-derived canopy % N and measured canopy properties. For example, Figure 3 shows the relationship between AVIRIS-predicted % N and observed forest composition at the study plots. For pixels classified in this manner as either 100% deciduous (% N ≥ 2.2) or 100% evergreen (% *N* ≤ 1.0), the image-based N concentration was used directly as the model input. For pixels classified as mixed (% N between 1.0 and 2.2), the canopy nitrogen concentration of each component, deciduous or evergreen, was determined from a similar empirical relationship, shown in Figure 4, between whole-canopy % N and the measured % *N* of each cover type. Parameter values for LMA and leaf retention time were determined for each forest type using data from field measurements at BEF (Smith and Martin 2001). Pixels classified as mixed were run for each vegetation type and the final output value was calculated as a weighted average of the two model runs, based on the estimated proportion of deciduous or evergreen composition for that pixel.

Results and Discussion

Stand Productivity and Canopy *N* Concentrations

Measured wood production at BEF ranged from 217 to 502 g m^{-2} $year^{-1}$ with a mean of 369 g m^{-2} $year^{-1}$ (n = 39). Areas of low productivity corresponded with higher elevations and sites

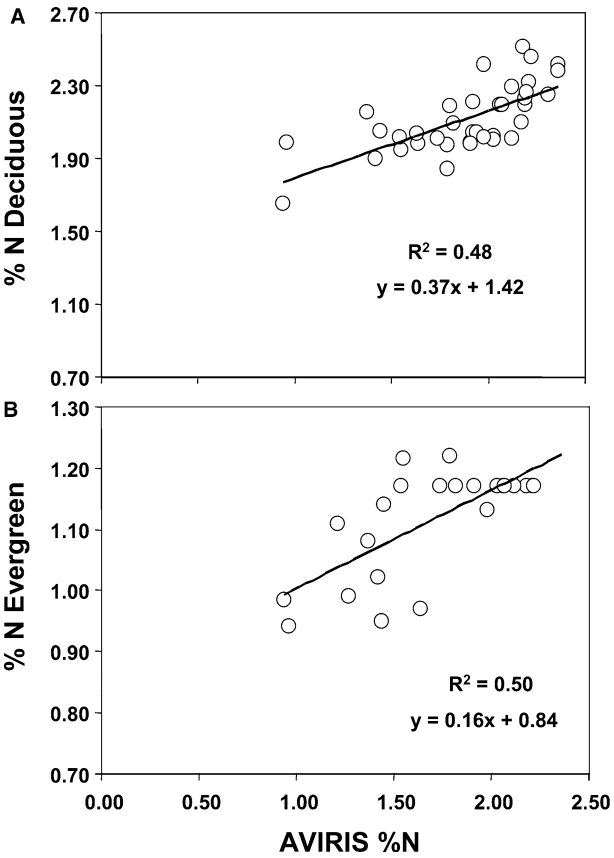

Figure 4. Measured foliar *N* concentration for (**a**) deciduous and (**b**) evergreen components of field plots in relation to the plot-level mean value estimated using AVIRIS.

with shallow soils dominated by needle-leaved evergreens (red spruce and hemlock). Mid-range values represent areas of mixed deciduous and evergreen forest (hemlock, red maple, American beech) on either coarse-textured or poorly drained soils. The highest values represent either mature deciduous forests comprised of sugar maple, beech, white ash, and yellow birch growing on fine textured, glacial till soils or early-successional deciduous stands dominated by pin cherry and paper birch. On plots that included leaf litterfall collections, foliar production ranged from 51 to 267 g m^{-2} $year^{-1}$ with a mean of 179 g m^{-2} $year^{-1}$. Aboveground net primary production (ANPP), the sum of wood and foliar production, ranged from 280 to 752 g m^{-2} $year^{-1}$ with a mean of 514 g m^{-2} $year^{-1}$.

Canopy-level N concentrations (g *N* 100 g^{-1} dry leaf biomass) varied more than twofold across sites, differing in both mean and range among deciduous and evergreen forest types. Among deciduous stands, canopy N ranged from 1.54 to 2.46% in 1997

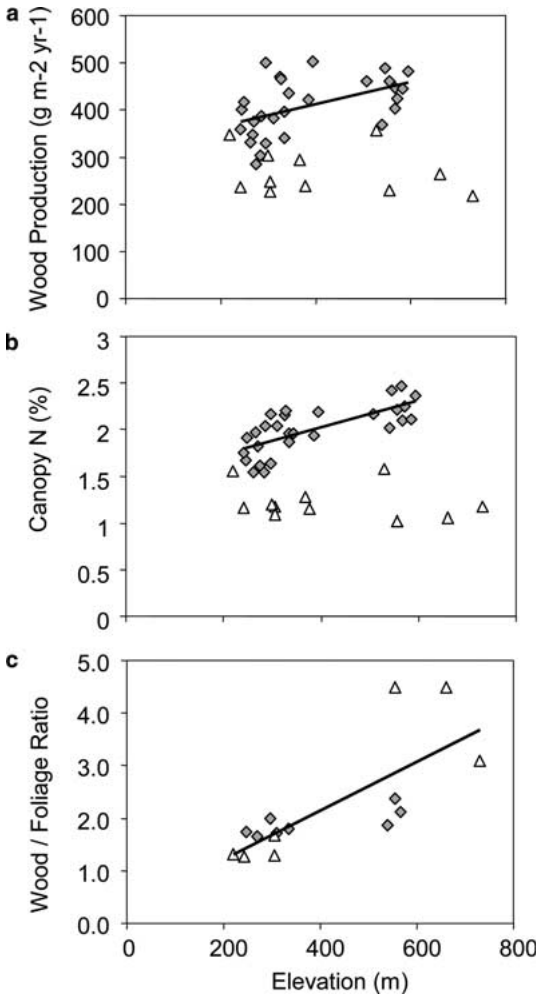

Figure 5. Elevation trends for (**a**) wood production, (**b**) foliar *N* concentrations and (**c**) the ratio of wood to foliage production. *Shaded diamonds* are plots dominated by deciduous species and *open triangles* are plots dominated by evergreens.

(n = 28, mean = 2.00%) and from 1.55 to 2.38% in 2000 (n = 10, mean = 1.92%). Among needle-leaved evergreen stands, canopy N ranged from 1.02 to 1.58% in 1997 (n = 11, mean = 1.22%) and from 1.06 to 1.49% in 2000 (n = 9, mean = 1.26%). Although foliar N concentrations can vary by as much as 20% between years in some temperate forests of this region (Magill and others 2000), between-year correlation in N concentration among the plots at BEF has been shown to be strong and of a much narrower range (R^2 = 0.86, SEE = 0.17, CV = 10%; Smith and others 2003).

Elevational Patterns

Over the elevation range sampled, there was a significant increase in wood production with increasing elevation for plots dominated by broad-leaf deciduous species (R^2 = 0.28, $P < 0.01$), a trend that mirrored a similar correlation between elevation and canopy N concentrations (R^2 = 0.52, $P < 0.01$, Figures 5a and b). This result was surprising and counters the generally-accepted pattern for the northeast study region. An often-cited example is the work by Whittaker and others (1974), who reported a decline in growth with elevation for both wood production and NPP for deciduous forests at Hubbard Brook. Although Hubbard Brook is within approximately 50 km of BEF and has similar species composition, this contrast may be due to differences in the elevation ranges sampled. At BEF, the deciduous stands sampled for this study ranged from 220 to 600 m and the lower portion of this range was primarily responsible for the observed trend in wood production. In contrast, data from Whittaker and others (1974) were taken from 550 to over 750 m. Similarly, on Whiteface Mountain in New York State, Joshi and others (2003) reported decreasing productivity with elevation, but the sites they examined were all located above 600 m.

One interpretation of these results is that there is a shift in the importance of moisture versus temperature limitations from low to high elevations within the region. Although such a shift is common in regions with greater topographic variability or of more arid climatic conditions, it has not been widely regarded in the northeastern U.S. Elevational increases in water availability result from several factors in the northeast, including increased precipitation, a decrease in transpiration caused by lower temperatures, and the tendency for mid-elevation soils to be derived from deeper deposits of fine-textured glacial till (Leak 1982). Supporting this interpretation, Federer (1982) used a forest hydrology model to estimate the frequency and intensity of drought events in New Hampshire forests and concluded that forests in low-elevation areas probably experience water deficits in most years.

Alternatively, the trend for deciduous species at BEF could stem solely from the elevational increase in foliar N concentrations and the effect this is expected to have on photosynthetic rates (Reich and others 1995). The reasons for this foliar N pattern are unclear, although a similar result was recently reported for sugar maple (Aber and others 2003). Additionally, a pattern of increasing foliar N with decreasing latitude and mean July temperatures was reported by Yin (1993), who suggested that plants in cold environments allocate greater amounts of N to leaves as a compensation for

Table 2. Summary Statistics for Partial Least Squares (PLS) Regression of Forest Canopy Nitrogen Concentration with AVIRIS and Hyperion Spectral Response, Bartlett Experimental Forest, New Hampshire, USA

		Calibration			Validation		
	PLS Factors	R^2	*SEC*	*Bias*	R^2	*RMSEP*	*Bias*
AVIRIS	3	0.83	0.17	0.00	0.79	0.19	0.00
HYPERION	3	0.82	0.17	0.00	0.60	0.25	0.00

suboptimal temperatures. It is also possible, if not likely, that changes in moisture availability and canopy nitrogen are not independent, but rather, that water status has an indirect effect on canopy N through its long-term role in organic matter production, decomposition and soil nitrogen availability (for example, Aber and others 1990; Schimel and others 1996; Bohlen and others 2001).

For evergreen-dominated stands, elevation was not correlated with either canopy N concentration or wood production, but was negatively correlated with foliar production ($R^2 = 0.80$, $P < 0.001$), a trend that was not observed in deciduous stands. A result of these contrasting elevation patterns—increasing wood growth for deciduous stands versus decreasing foliar growth for evergreen stands—was that both functional groups exhibited a similar positive relationship between elevation and the ratio of wood to foliar production (Figure 5c, $R^2 = 0.56$, $P < 0.001$). If we interpret this ratio as an indication of foliar growth efficiency (mass of wood produced per unit investment in foliage), this trend marks an increase in efficiency with elevation for both cover types. In deciduous stands, this is most likely caused by the effects of increased water availability and foliar N concentrations on canopy photosynthesis. In evergreen stands, this pattern is more likely driven by variation in leaf retention time, which affects carbon use efficiency by altering the annual investment in foliage per unit standing foliar biomass. Although we did not estimate evergreen leaf longevity on the BEF study plots, there is abundant evidence for increasing needle-retention time with increasing elevation, both within species (for example, Ewers and Schmid 1981; Schoettle 1990; Reich and others 1996) and between species occurring at different elevations within the study area (Reich and others 1995; Smith and Martin 2001).

Spatial Patterns in Predicted Productivity

Results of PLS regressions relating spectral data from AVIRIS and Hyperion to measured canopy % N are summarized in Table 2. For both sensors, the best models contained three factors derived from the spectral data. Figure 6 shows predicted versus observed canopy N concentrations for the calibration and validation models from each sensor. Hyperion estimates, though of lower accuracy than AVIRIS estimates, are surprisingly robust given Hyperion's much lower signal-to-noise and the temporal offset between field data collection and image acquisition for the study site.

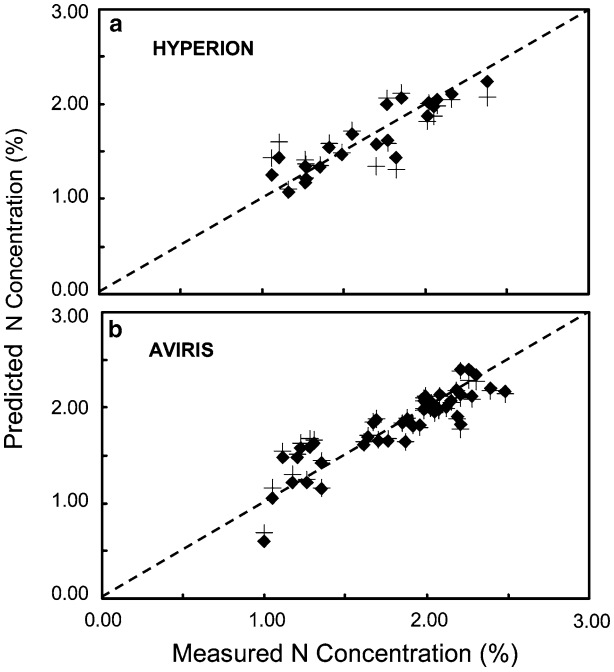

Figure 6. Predicted versus observed canopy nitrogen concentration based on PLS regression models using (**a**) HYPERION and (**b**) AVIRIS absorbance data. In both panels *diamonds* represent the calibration model and *crosses* represent the validation model. Dashed lines represent the 1:1 relationship.

Figure 7 illustrates the result of PnET-II simulations for the 5 × 5 km study area, using AVIRIS-derived canopy N concentrations at 17 m spatial resolution, overlaid onto a hill-shaded DEM. Predicted NPP ranged from less than 700 g m^{-2} $year^{-1}$ to greater than 1300 g m^{-2} $year^{-1}$ with a mean of 951 g m^{-2} $year^{-1}$. Elevation trends in predicted

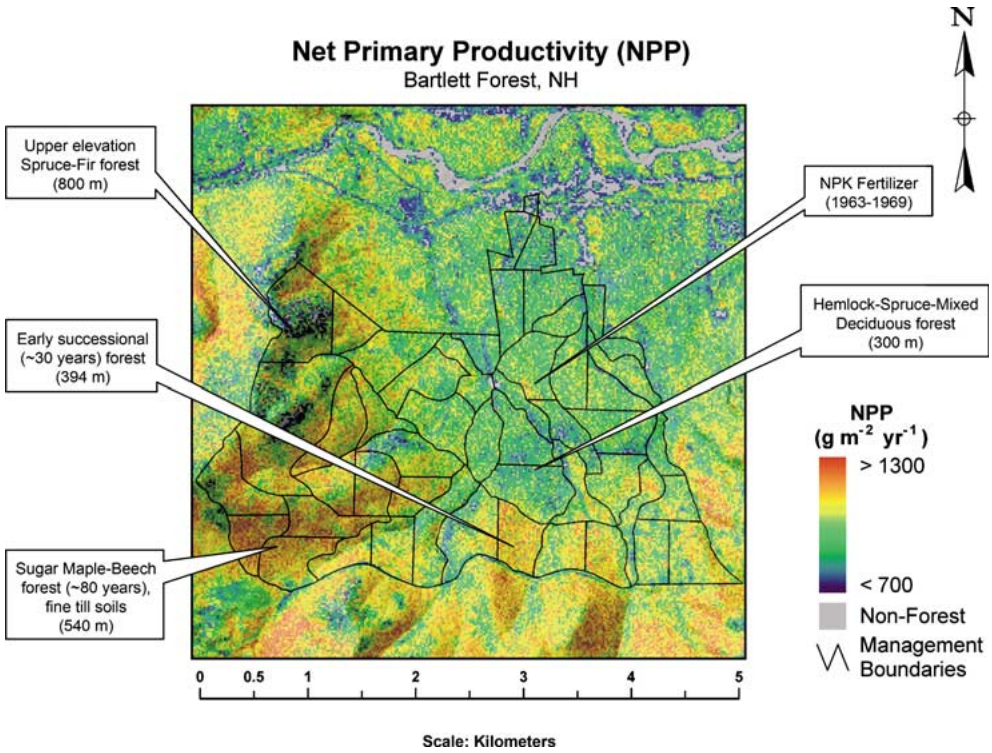

Figure 7. Hill-shaded map of predicted net primary productivity (NPP) generated by running PnET-II with AVIRIS-derived canopy nitrogen estimates. For mixed pixels, the ratio of deciduous to evergreen cover types and the foliar *N* concentration of each were estimated using empirically-derived relationships in Figures 3 and 4. *Callout boxes* highlight forest areas of differing productivity related to topographic position, stand age, and manipulative treatment (cutting, NPK fertilization).

NPP reflect a combination of the observed patterns for individual cover types and the fact that upper-elevation areas are dominated by evergreen species (red spruce, balsam fir and eastern hemlock). The shading in Figure 7 highlights the topography at BEF—for example, pale yellow and green areas in the northeastern portion of the image are low elevation and of mixed evergreen and deciduous species composition; small patches of blue and dark green in the northwest portion of the image are conifer-dominated areas near mountain summits (see Figure 7 callout boxes). The overall elevation trend is nonlinear, increasing from low to mid elevations and then decreasing at upper-elevation sites where evergreen stands become increasingly dominant.

Figure 7 also reveals interesting spatial patterns that were not evident from the more limited coverage of the plot-level data, but correspond to variation in species composition, soil type and forest management history, via their combined effects on the observed patterns of canopy nitrogen. For example, a number of high-productivity areas in the southeast (lower right) portion of BEF were subjected to timber harvests in the mid-1970's and, today, are largely composed of early successional species, such as pin cherry and paper birch, characterized by high foliar N concentrations. Similarly, in the northeastern (upper right) portion of BEF, which is mostly made up of mid successional stands consisting of red maple, American beech, paper birch, hemlock and scattered white pine, a small patch of high productivity forest that stands out from its immediate surroundings (see Figure 7 callout box) corresponds to the location of an experimental harvest and fertilization treatment conducted in 1968 (L.O. Safford, personal communication). After clearcutting, a 4 ha area was subjected to broadcast application of various combinations of limestone and commercial NPK fertilizer, treatments that had significant effects on foliar nutrient concentrations and tree growth increment in the years following the experiment (Safford 1973). It is unclear whether the elevated present-day N concentrations detected by AVIRIS reflect the singular effects of an early successional forest community or the combined effects of species composition and prolonged site enrichment from fertilization.

Areas of similarly high productivity in the southwest portion of BEF correspond to mature sugar maple and American beech stands growing on fine till soils (Leak 1982). Although foliar N values for these species are generally lower than that of pin cherry and other early successional species present in recent clearcuts, they can attain similar levels on rich sites with minimal history of prior disturbance (Ollinger and others 2002).

Plot-Level Validation of Productivity Estimates

The accuracy of productivity estimates derived using remotely-sensed canopy N was evaluated by comparing model predictions of wood production and ANPP for individual field plots with the field-measured estimates. Although validation for total NPP would be ideal, there have been no measurements of belowground production for the sample plots at BEF. For wood production, model predictions corresponded reasonably well with measured values (Figure 8). The R^2 of predicted versus observed values using AVIRIS-derived foliar N data ($n = 39$) was 0.74 with a standard error of the estimate (SEE) of 44.0 g m^{-2} $year^{-1}$, or 11.9% of measured mean woody biomass production. Predictions based on Hyperion-derived foliar N ($n = 19$) had an R^2 for predicted versus observed values of 0.70 with a standard error of 49.3 g m^{-2} $year^{-1}$ or 13.4% of measured mean woody biomass production.

In addition to the scatter around predicted versus observed regression lines, comparison with the 1:1 lines in Figure 8 show that model predictions overestimated measured values by approximately 15%. This bias could arise from errors in the model, error in the input parameters used in the simulations, or differences between the specific plant tissues included in the model versus those captured by the field measurements. In PnET, wood production is calculated as the difference between total NPP and biomass allocated to leaves and fine roots. As a result, predicted wood production includes woody root tissue as well as aboveground stem and branch production, whereas observed wood production was derived from allometric equations that included aboveground woody tissues, but not woody roots. Whittaker and others (1974) estimated that woody root biomass at Hubbard Brook was approximately 10% of total woody biomass, suggesting that the difference between aboveground versus total wood production could account for at least part of the apparent discrepancy.

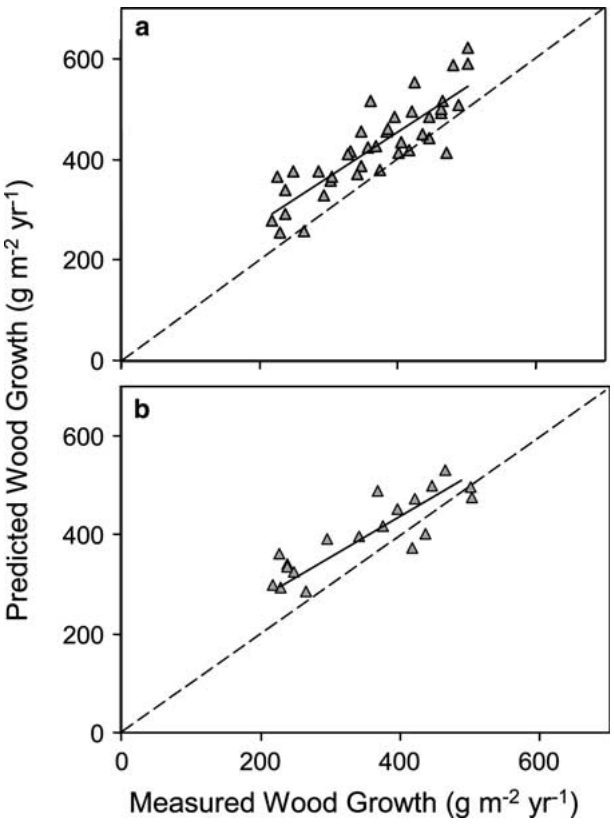

Figure 8. Predicted versus observed wood growth for simulations using (**a**) AVIRIS-derived canopy *N* data and (**b**) Hyperion-derived canopy *N* data. Predicted values represent image pixels corresponding to the location of field plots. *Solid lines* represent predicted versus observed regressions and *dashed lines* show the 1:1 relationship.

Discrepancies between the plant components included in measured versus modeled components of productivity are a common problem in this type of study because many components of NPP are difficult to measure directly (for example, tissues lost to herbivory, woody litterfall, root exudates, VOC emissions). Clark and others (2001) attempted to summarize these measurement errors and concluded that most of the challenges associated with productivity measurements result in underestimation, rather than overestimation, and collectively, can cause systematic downward bias.

Another source of error in predicted values corresponded to errors in the remotely-derived canopy nitrogen. This is seen in Figure 9, which shows a weak, but positive correlation between the ratio of predicted to observed wood growth and the ratio of predicted to observed canopy N. In other words, the model tended to overestimate wood growth in stands where AVIRIS overestimated canopy N and vice versa. The importance of canopy N as a driver

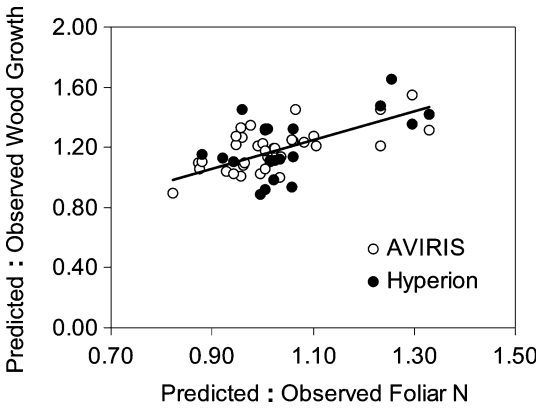

Figure 9. The ratio of predicted to observed wood growth in relation to the ratio of predicted to observed canopy nitrogen. *Open circles* show the trend obtained using AVIRIS-derived canopy *N*; *closed circles* show the trend using Hyperion-derived canopy *N*.

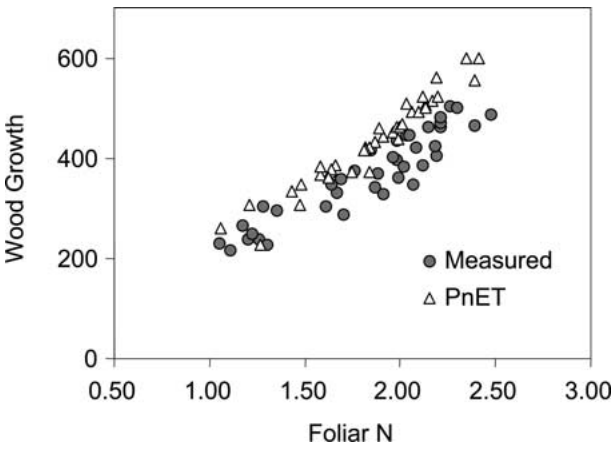

Figure 10. Predicted and observed relationships between foliar N concentration and wood growth (g m^{-2} $year^{-1}$). The predicted trend shows AVIRIS-derived canopy *N* in relation to modeled wood growth; the observed trend shows measured canopy *N* in relation to measured wood growth.

for patterns of growth at BEF is indicated in Figure 10, which shows the relationship between canopy N and wood production, both in the measured field data and as predicted by PnET-II. Although Figure 10 also shows the small tendency for model predictions to overestimate measured values, the predicted and observed values are qualitatively very similar. This suggests that the leaf-level foliar N–photosynthesis relationship used in the model translates to similar patterns of carbon gain for whole forest canopies.

Figure 11 shows the relationship between predicted ANPP from PnET-II using AVIRIS-estimated canopy N and observed values for the plots where foliar litter production was also measured. The overall agreement is similar to that for wood production (R^2 = 0.77, SEE = 66.1, or 12.6% of mean measured ANPP), but with a slight bias towards overestimation at the low end of the range. This pattern is caused by an overestimation of leaf production for low productivity evergreen stands relative to the litterfall-derived estimates. This discrepancy is probably related to the previously-discussed issue of leaf longevity (Results and Discussion; Elevational Patterns) in that leaf retention time is known to increase in low-productivity environments (Reich and others 1999b). This generally corresponds to reduced foliar production because a smaller fraction of canopy biomass requires replacement on a year-to-year basis.

Effects of Alternative Foliar N Data Sources

The relationship between canopy N and forest productivity at BEF suggests that the ability to estimate canopy N using remote sensing should improve growth prediction capabilities substantially. However, because remotely-derived canopy N data have not been widely available, the specific level of enhancement relative to other, more commonly available data sources has not previously been assessed. To address this question, we performed two additional sets of simulations for the 39 field measurement plots. First, to determine how well the model would perform using the most accurate canopy N data available, we performed model simulations for each plot using species-specific canopy N values from direct field measurements. For plots that had more than one cover type, we ran each cover type separately and weighted the resulting predictions according to observed deciduous-to-evergreen ratios. These simulations relied entirely on field-measured data and represented the most accurate parameter set we had available. For simplicity, we refer to results from these simulations as the **Measured-N** model predictions.

For a second set of simulations, we sought to assess the accuracy of predictions that would be expected if plot-level canopy N data were not available. An approach used by many investigators in such cases has been to use forest cover type maps obtained from more commonly-available sensors (for example, Landsat TM) with vegetation parameters held constant within each cover type (for example, Ollinger and others 1998; Pan and others 2002). To represent this type of analysis, we grouped all plots into deciduous, evergreen or mixed forest types. Stands treated as deciduous or

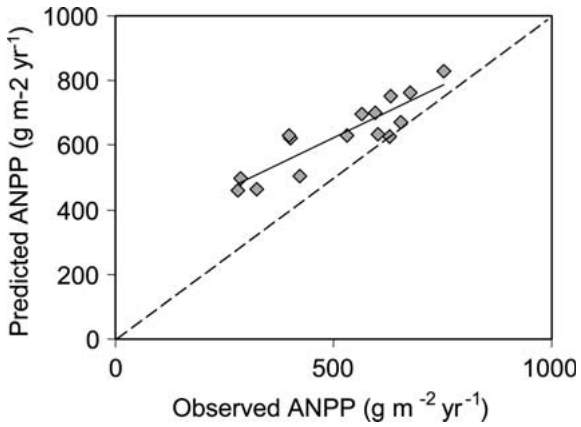

Figure 11. Predicted versus observed aboveground net primary production (ANPP, $R^2 = 0.77$, SEE = 65.1 g m^{-2} $year^{-1}$). Predictions were based on AVIRIS-derived canopy *N* inputs; measured values were calculated as wood growth plus annual leaf litterfall. The *solid line* represents the predicted versus observed regression and the dashed line shows the 1:1 relationship.

evergreen consisted of over 65% of a single cover type and mixed stands contained between 35 and 65% of each. For each cover type, we used its mean canopy % N value, obtained from field measurements from across BEF. For mixed stands, we ran each cover type separately and weighted the resulting predictions using a 50:50 deciduous-to-evergreen ratio. These simulations represent a relatively common scenario in which aggregated vegetation data are combined with broad cover type classifications. Results from these simulations as referred to as the **Mean-N** model predictions.

Comparisons of predictions generated from these analyses are shown in Figure 12. Predicted wood growth under the **Measured-N** simulations (Figure 12a) showed the best overall agreement with measured values and represented an improvement over predictions generated using remotely-derived canopy N ($R^2 = 0.79$, SEE = 39.4, or 10.7% of the mean measured wood production). The predicted mean for all plots (422 g m^{-2} $year^{-1}$) was similar to that obtained using remotely-sensed canopy N (427 g m^{-2} $year^{-1}$ using AVIRIS; 403 g m^{-2} $year^{-1}$ using Hyperion) and showed the same tendency towards slight over-prediction.

Predicted wood growth obtained under the **Mean-N** simulations (Figure 12b) agreed reasonably well with results from other simulations in terms of the overall mean (415 g m^{-2} $year^{-1}$), but showed poor agreement with measured values on a plot-by-plot basis ($R^2 = 0.37$, SEE = 67.5, or 18.3% of the mean measured wood production). This was caused by a combination of the aggregated canopy

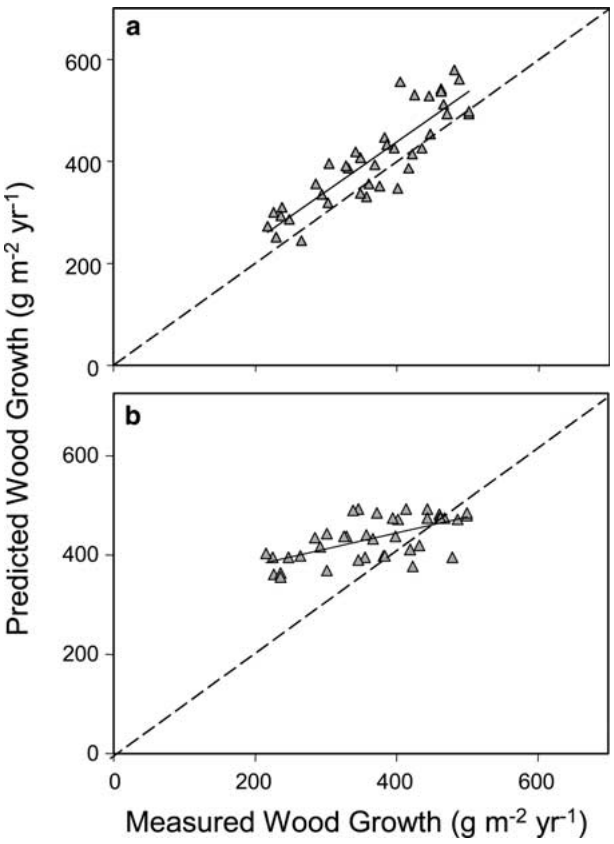

Figure 12. Predicted versus observed wood growth using two alternative methods of obtaining foliar *N* model input data. In **(a)**, PnET-II was run for individual field plots using species-specific foliar *N* values from samples collected at each plot ($R^2 = 0.79$, SEE = 39.4 g m^{-2} $year^{-1}$). These results correspond to the 'Measured-N' predictions referred to in the text. In **(b)** PnET-II was run using mean % *N* values for deciduous and evergreen species, averaged over all plots at Bartlett ($R^2 = 0.37$), representing a typical modeling scenario where plot-by-plot foliar *N* estimates were unavailable. These results correspond to the '**Mean-N**' predictions referred to in the text. *Dashed lines* show the 1:1 relationships.

N values and fixed deciduous-to-evergreen ratios used in the model runs, both of which tend to bias predictions towards the overall population mean. The differences between the **Measured-N** simulations (Figure 12a) and the **Mean-N** simulations (Figure 12b) suggest substantial and ecologically important fine-scale variation in canopy N that is not accurately captured by using mean values for a given cover type.

Canopy N versus Structural Indices of Forest Productivity

Results from this analysis indicate that canopy nitrogen provides an effective integrator of factors

affecting NPP across heterogeneous forested landscapes. However, it is also worth considering other canopy properties that have been examined for this purpose by other investigators or in other ecosystems. Although the importance of foliar nutrients is not new to ecologists, the majority of effort to characterize NPP spatial patterns have focused instead on methods for measurement and detection of structural properties such as leaf area index (LAI, for example, Tucker and Sellers 1986; Running and others 1989; Lui and others 1997; Gower and others 1999). There are at least three reasons for this: (1) LAI provides a useful measure of the amount of light-harvesting foliage available for photosynthesis (for example, Gower and others 1999); (2) the amount of photosynthetically-active radiation absorbed by plant canopies (APAR) is often assumed to be more important than the efficiency with which individual leaves convert captured light into new photosynthate (Myneni and others 1997); and (3) methods for estimating LAI and APAR have been available for some time using broad-band optical remote sensing (Tucker and Sellers 1986).

To date, relationships among LAI, APAR and forest growth have been most effectively demonstrated in evergreen forests and across large resource gradients where substantial variation in LAI or canopy cover fraction occur (for example, Vose and Allen 1988; Gower and others 1992; Matson and others 1994; Fassnacht and Gower 1997). This approach appears to be more limited at finer spatial scales and within regions where moisture regimes and LAI are less variable, but where variation in growth nevertheless occurs due to variation in nutrient availability and photosynthetic capacity. Difficulties with methods based solely on LAI stem from the fact that relationships between LAI and absorbed radiation are asymptotic, and their relevance to variation in growth tends to saturate in dense, closed canopy systems. In other words, at high LAI, the incremental change in light absorption and carbon fixation associated with the production of additional foliage decreases. This pattern has been well documented and stems from the fact that, as leaf area increases, the amount of radiation intercepted by additional leaf layers declines exponentially due to increased self-shading (Gower and others 1993; Reich and others 1999a). The result is that relationships among LAI, APAR and productivity eventually become saturated and, at LAI values above 3 or 4, these variables become increasingly decoupled (for example, see Turner and others 1999). In many systems, this is a relatively minor issue, but in closed-canopy forests, it can present a substantial challenge.

Although we did not specifically address LAI in this study, Smith and others (2002) showed that productivity across the White Mountains, NH was correlated with LAI in conifer forests, but not in deciduous forests (where LAI varied little) and that LAI was a weaker correlate overall than foliar N. This suggests that productivity in the temperate forest ecosystems of the White Mountains is not driven simply by patterns of radiation absorption, but that differences in canopy nutrition exert an important, if not dominant, influence. Despite these findings, the generality of canopy *N*–productivity relationships have not been widely tested in other regions and the relative amount of spatial variability that can be captured across a range of ecosystems via LAI versus foliar N remains unclear. At best, the examples described above allow us to speculate that LAI may be responsible for a greater amount of variability in evergreen forests and across broad resource gradients, whereas the influence of canopy N becomes more important in deciduous forests and at finer spatial resolutions where site factors such as disturbance history and species composition are important.

It is also important to consider that a number of productivity models generate predictions using a combination of remotely-sensed estimates of LAI and APAR along with estimates of canopy light use efficiency (for example, Potter and others 1993; Prince and Goward 1995; Ruimy and others 1994; Running and others 2000). These production efficiency models are based on the equation NPP = ε *x* APAR, where ε represents maximum light use efficiency (g MJ^{-1}), adjusted for suboptimal climatic conditions. Production efficiency models are appealing for broad-scale analyses because of the availability of APAR estimates from multi-spectral sensors. However, a persistent challenge has been the lack of predictive understanding concerning factors controlling variation in ε, both within and among vegetation types. As a consequence, most of these models either assume a global mean value of ε for all vegetation types (for example, Potter and others 1993) or rely on look-up tables that assign single values for individual biomes (for example, Running and others 2000). Because published values of ε vary widely (Ruimy and others 1994), these solutions are unsatisfying in that an important source of variation remains unaccounted for.

A recent meta-analysis by Green and others (2003) offers a potential solution to this problem and may reconcile differences in approaches based on LAI versus canopy N. The authors compiled published values of ε and a variety of other canopy traits from an array of C3 plant communities,

including deciduous and evergreen tree species, and herbaceous species consisting of grasses, forbs and legumes. Their results showed that, of all factors considered, the variable that explained the greatest amount of variation in ε was the mass-based leaf nitrogen concentration. If we assume, then, that LAI affects the component of NPP that is driven by variation in light absorption, and that canopy N represents the efficiency with which light is converted into new photosynthate, development of independent methods to assess patterns of LAI and canopy N across a range of spatial scales would be a huge benefit for studies of terrestrial productivity.

Conclusions

This analysis suggest that variation in canopy N concentrations across heterogeneous landscapes can serve as an integrator of underlying factors that influence forest growth rates and that the role of N concentrations as a control on leaf-level photosynthesis also applies to C fixation by whole forest canopies. This supports the findings of several prior field studies (Bauer and others 1997; Smith and others 2002) as well as a recent meta-analysis that pointed to foliar N as a key source of variability in canopy light use efficiency across a range of ecosystem types (Green and others 2003).

In the present study, we extended field-based productivity estimates for BEF to total net primary production through use of a spatially-distributed ecosystem model and investigated the degree to which landscape-scale spatial patterns were affected by factors such as elevation, forest composition and forest management. We also evaluated the effects on model performance of different sources of canopy N input data; plot-level field measurements, estimates from two hyperspectral remote sensing instruments, and aggregated values for deciduous and evergreen canopies. Although use of field-measured canopy N data provided the highest absolute prediction accuracy, remotely-derived canopy N estimates from NASA's AVIRIS and Hyperion sensors provided growth estimates that were nearly as accurate in terms of agreement with plot-level measurements and, most importantly, allowed predictions to be extended over the larger surrounding landscape. Data from both sensors resulted in predictions that were substantial improvements over those generated using aggregated canopy N inputs.

Our results suggest that efforts to detect fine-scale patterns of forest productivity and carbon uptake in northeastern forest ecosystems will depend on the quality of canopy N data and that the success of remote sensing-based methods that fail to capture patterns of canopy N will be limited. Expanding the utility of the approach used in this analysis will require future investment in a number of areas. First, although imaging spectroscopy appears to hold considerable promise for ecosystem analyses, data are still not widely available and more generalizeable algorithms for detection of vegetation properties have yet to emerge. Second, while patterns of aboveground production were shown to be characterized with a reasonable level of confidence, our confidence in predicted patterns of belowground production is far lower and will require that additional effort be directed towards belowground measurements.

Acknowledgements

This study was conducted with supported from the NASA Carbon Cycle Science Program (CARBON-0000-1234), and the National Institute for Global Environmental Change (UNH/901214-02). We also received support from the USDA Forest Service Northeastern Research Station (NE-4155) and the USDA Forest Service Southern Global Change Program. We thank Mary Martin, Julian Jenkins, Lucie Plourde and Rita Freuder for assistance with image processing and ecosystem modeling and we thank Shannon Cromley, Rich Hallett, Alison Magill, Jim Muckenhoupt and Gloria Quigley for assistance with field data collection and laboratory analysis. Finally, we are grateful to John Aber and John Pastor for their thoughtful comments on earlier versions of this manuscript.

References

Aber JD, Melillo JM, McClaugherty CA. 1990. Predicting long-term patterns of mass loss, nitrogen dynamics, and soil organic matter formation from initial fine litter chemistry in temperate forests. Can J Bot 68:2201–8.

Aber JD, Federer CA. 1992. A generalized, lumped-parameter model of photosynthesis, evapotranspiration and net primary production in temperate and boreal forest ecosystems. Oecologia 92:463–74.

Aber JD, Ollinger SV, Federer CA, Reich PB, Goulden ML, Kicklighter DW, Melillo JM, Lathrop RG. 1995. Predicting the effects of climate change on water yield and forest production in the northeastern US. Clim Res 5:207–22.

Aber JD, Reich PB, Goulden ML. 1996. Extrapolating leaf CO_2 exchange to the canopy: a generalized model of forest photosynthesis validated by eddy correlation. Oecologia 106:257–65.

Aber JD, Goodale CL, Ollinger SV, Smith ML, Magill AH, Martin ME, Hallett RA, Stoddard JL, NERC Participants. 2003. Is nitrogen deposition altering the nitrogen status of northeastern forests? Bioscience 53(4):375–89.

Asner GP. 1998. Biophysical and biochemical sources of variability in canopy reflectance. Remote Sens Environ 64:234–53.

Barry P. 2001. EO-1 Hyperion Science Data User's Guide. Redondo Beach, CA: TRW Corporation, Publication HYP.-TO.01.077, p 65.

Bauer G, Schulze E-D, Mund M. 1997. Nutrient contents and concentrations in relation to growth of Picea abies and Fagus sylvatica along a European transect. Tree Physiol 17:777–86.

Bolster KL, Martin ME, Aber JD. 1996. Determination of carbon fraction and nitrogen concentration in tree foliage by near infrared reflectance: a comparison of statistical methods. Can J Forest Res 26:590–600.

Boegh E, Soegaard H, Broge N, Hasager CB, Jensen NO, Schelde K, Thomsen A. 2002. Airborne multispectral data for quantifying leaf area index, nitrogen concentration, and photosynthetic efficiency in agriculture. Remote Sens Environ 81(2–3):179–93.

Bohlen PJ, Groffman PM, Driscoll CT, Fahey TJ, Siccama TG. 2001. Plant-soil-microbial interactions in a northern hardwood forest. Ecology 82(4):965–78.

Bousquet P, Peylin P, Ciais P, Le Quéré C, Friedlingstein P, Tans P. 2000. Regional changes in carbon dioxide fluxes of land and oceans since 1980. Science 290:1342–6.

Burke IC, Lauenroth WK, Parton WJ. 1997. Regional and temporal variation in net primary production and nitrogen mineralization in grasslands. Ecology 78(5):1330–40.

Clark DA, Brown S, Kicklighter DW, Chambers JW, Thomlinson JR, Ni J. 2001. Measuring net primary production in forests: concepts and field methods. Ecol Appl 11:356–70.

Cole DW. 1995. Soil nutrient supply in natural and managed forests. Plant Soil 169:43–53.

Coops NC, Waring RH. 2001. The use of multiscale remote sensing imagery to derive regional estimates of forest growth capacity using 3-PGS. Remote Sens Environ 75:324–34.

Craine J, Bond W, Lee WG, Reich PB, Ollinger SV. 2003. The resource economics of chemical and structural defenses across nitrogen supply gradients. Oecologia 137(4):547–56.

Curran PJ, Kupiec JA, Smith GM. 1997. Remote sensing the biochemical composition of a slash pine canopy. IEEE Trans Geosci Remote Sens 35:415–20.

Ellsworth DS, Reich PR. 1993. Canopy structure and vertical patterns of photosynthesis and related leaf traits in a deciduous forest. Oecologia 96:169–78.

Ewers FW, Schmid R. 1981. Longevity of needle fascicles of *Pinus longaeva* (Bristlecone Pine) and other North American pines. Oecologia 51:107–15.

Fan S, Gloor M, Mahlman J, Pacala S, Sarmiento J, Takahashi T, Tans P. 1998. A large terrestrial carbon sink in North America implied by atmospheric and oceanic carbon dioxide data and models. Science 282:442–6.

Fassnacht KS, Gower ST. 1997. Interrelationships among the adaphic and stand characteristics, leaf area index, and aboveground net primary production of upland forest ecosystems in north central Wisconsin. Canadian Journal of Forest Research. 27:1058–1067.

Federer CA. 1982. Frequency and intensity of drought in New Hampshire forests: evaluation by the BROOK model. In: Applied Modeling in Catchment Hydrology, Proceedings of the international symposium on rainfall-runoff modeling, May 1981, Littleton (CO): Water Resources Publications.

Field C, Mooney HA. 1986. The photosynthesis—nitrogen relationship in wild plants. In: Givnish TJ, Ed. On the Economy of Plant Form and Function. Cambridge: Cambridge University Press. p 25–55.

Fournier RA, Guindon L, Bernier PY, Ung CH, Raulier F. 2000. Spatial implementation of models in forestry. Forestry Chron 76(6):929–40.

Gao B, Heidebrecht KB, Goetz A. 1993. Derivation of scaled surface reflectances from AVIRIS data. Remote Sens Environ 44:165–78.

Gower ST, Vogt KA, Grier CC. 1992. Carbon dynamics of Rocky Mountain Douglas Fir: influence of water and nutrient availability. Ecol Monogr 62:43–65.

Gower ST, McMurtrie RE, Murty D. 1996. Aboveground net primary production decline with stand age: potential causes. Trends Ecol Evol 11(9):378–82.

Gower ST, Kucharik CJ, Norman JM. 1999. Direct and indirect estimation of leaf area index, f(APAR), and net primary production of terrestrial ecosystems. Remote Sens Environ 70(1):29–51.

Green RO, Eastwood ML, Sarture CM, Chrien TG, Aronsson M, Chippendale BJ, Faust JA, Pavri BE, Chovit CJ, Solis M, Olah MR, Williams O. 1998. Imaging spectrometry and the airborne visible/infrared imaging spectrometer (AVIRIS). Remote Sens Environ 65:227–48.

Green RO, Pavri B, Faust J, Williams O. 1999. AVIRIS radiometric laboratory calibration, inflight validation, and a focused sensitivity analysis in 1998. In: Green RO, Ed. Summaries of the Eighth JPL Airborne Earth Sciences Workshop, JPL Publication 99–17. Pasadena (CA): National Aeronautics and Space Administration. p 161–75.

Green DS, Erickson JE, Kruger EL. 2003. Foliar morphology and canopy nitrogen as predictors of light-use efficiency in terrestrial vegetation. Agric Forest Meteorol 115:163–71.

He HS, Mladenoff DJ, Radeloff VC, Crow TR. 1998. Integration of GIS data and classified satellite imagery for regional forest assessment. Ecol Appl 8(4):1072–83.

Hocker HW, Early DJ. 1983. Biomass and leaf area equations for northern forest species. Research Report 102. Durham (NH): New–Hampshire Agricultural Experiment Station.

Houghton R, Hackler J, Lawrence K. 1999. The U.S. carbon budget: contributions from land-use change. Science 285:574–8.

Hrushcka WR. 1987. Data analysis: wavelength selection methods. In: Williams P, Norris K, Eds. Near-Infrared Technology in the Agricultural and Food Industries. St. Paul (MN) USA: American Association of Cereal Chemists, Inc.

Joshi AB, Vann DR, Johnson AH, Miller EK. 2003. Nitrogen availability and forest productivity along a climosequence on Whiteface Mountain, New York. Can J Forest Res. 33(10):1880–91.

Jupp DPL, Datt B, Lovell J, King E. 2002. EO-1/Hyperion data workshop notes. CSIRO Office of Space Science & Applications, Earth Observation Centre, Canberra, Australia.

Kimball JS, Keyser AR, Running SW, Saatchi SS. 2000. Regional assessment of boreal forest productivity using an ecological process model and remote sensing parameter maps. Tree Physiol 20(11):761–75.

Kokaly RF, Despain DG, Clark RN, Livoa KE. 2003. Mapping vegetation in Yellowstone National Park using spectral feature analysis of AVIRIS data. Remote Sens Environ 84:437–56.

Kramer R. 1998. Chemometric techniques for quantitative analysis. New York: Marcel Dekker, Inc. p 203.

Leak WB. 1982. Habitat mapping and interpretation in New England. USDA Forest Service Research Paper NE-496. Broomall (PA): Northeastern Forest Experiment Station.

Leith H. 1975. Modeling the primary productivity of the world: In: Leith H, Whittaker RH, Eds. Primary Productivity of the Biosphere, Berlin Heidelberg. New York: Springer. p 237–63.

Liu J, Chen JM, Cihlar J, Park WM. 1997. A process-based boreal ecosystem productivity simulator using remote sensing inputs. Remote Sens Environ 62(2):158–75.

Magill AH, Aber JD, Berntson GM, McDowell WH, Nadelhoffer KJ, Melillo JM, Steudler PA. 2000. Long-term nitrogen additions and nitrogen saturation in two temperate forests. Ecosystems 3:238–53.

Martin ME, Aber JD. 1997. High spectral resolution remote sensing of forest canopy lignin, nitrogen and ecosystem processes. Ecol Appl 7:431–43.

Martin ME, Newman SD, Aber JD, Congalton RG. 1998. Determining forest species composition using high spectral resolution remote sensing data. Remote Sens Environ 65:249–54.

Matson P, Johnson L, Billow C, Miller J, Pu R. 1994. Seasonal patterns and remote spectral estimation of canopy chemistry across the Oregon transect. Ecol Appl 4(2):280–98.

Motzkin G, Wilson P, Foster DR, Allen A. 1999. Vegetation patterns in heterogeneous landscapes: the importance of history and environment. J Veg Sci 10(6):903–20.

Myneni RB, Nemani RR, Running SW. 1997. Estimation of global leaf area index and absorbed PAR-photosynthetically active radiation using radiative transfer models. IEEE Trans Geosci Remote Sens 35(6):1380–93.

O'Neill AL, Kupiec JA, Curran PJ. 2002. Biochemical and reflectance variation throughout a Sitka spruce canopy. Remote Sens Environ 80:134–42.

Ollinger SV, Aber JD, Federer CA, Lovett GM, Ellis JM. 1995. Modeling physical and chemical climate of the northeastern U.S. for a geographic information system. USDA Forest Service General Technical Report NE-191.

Ollinger SV, Aber JD, Federer CA. 1998. Estimating regional forest productivity and water yield using an ecosystem model linked to a GIS. Landscape Ecol 13:323–34.

Ollinger SV, Smith ML, Martin ME, Hallett RA, Goodale CL, Aber JD. 2002. Regional variation in foliar chemistry and soil nitrogen status among forests of diverse history and composition. Ecology 83(2):339–55.

Pan Y, McGuire D, Melillo JM, Kicklighter DW, Sitch S, Prentice IC. 2002. A biogeochemistry-based dynamic vegetation model and its application along a moisture gradient in the continental United States. J Veg Sci 13:369–82.

Pastor J, Aber JD, McClaugherty CA, Melillo JM. 1984. Aboveground production and N and P cycling along a nitrogen mineralization gradient on Blackhawk Island, Wisconsin. Ecology 65:256–68.

Pickett STA, Cadenasso ML. 1995. Landscape ecology—spatial heterogeneity in ecological systems. Science 269(5222):331–4.

Potter CS, Randerson JT, Field CB, Matson PA, Vitousek PM, Mooney HA, Klooster SA. 1993. Terrestrial ecosystem production—a process model-based on global satellite and surface data. Global Biogeochem Cycles 7:811–41.

Prince SD, Goward SN. 1995. Global Primary production: a remote sensing approach. J Biogeogr 22:815–35.

Reed RA, Finley ME, Romme WH, Turner MG. 1999. Aboveground net primary production and leaf-area index in early postfire vegetation in Yellowstone National Park. Ecosystems 2(1):88–94.

Reich PB, Kloeppel B, Ellsworth DS, Walters MB. 1995. Different photosynthesis—nitrogen relations in deciduous and evergreen coniferous tree species. Oecologia 104:24–30.

Reich PB, Oleksyn J, Modrzynski J, Tjoelker MG. 1996. Evidence that longer needle retention of spruce and pine populations at high elevations and high latitudes is largely a phenotypic response. Tree Physiol 16:643–7.

Reich PB, Grigal DF, Aber JD, Gower ST. 1997. Nitrogen mineralization and productivity in 50 hardwood and conifer stands on diverse soils. Ecology 78:335–47.

Reich PB, Turner DP, Bolstad P. 1999a. An approach to spatially distributed modeling of net primary production (NPP) at the landscape scale and its application in validation of EOS NPP products. Remote Sens Environ 70:69–81.

Reich PB, Ellsworth DS, Walters MB, Vose JM, Gresham C, Volin JC, Bowman WB. 1999b. Generality of leaf traits relationships: a test across six biomes. Ecology 80:1955–69.

Roberts DA, Gardener M, Church R, Ustin S, Scheer G, Green RO. 1998. Mapping chapparal in the Santa Monica mountains using multiple end member spectral mixture models. Remote Sens Environ 65:267–79.

Ruimy A, Saugier B, Dedieu G. 1994. Methodology for the estimation of terrestrial net primary production from remotely-sensed data. J Geophy Res 99:5263–83.

Running SW, Nemani RR, Peterson DL, Band LE, Potts DF, Pierce LL, Spanner MA. 1989. Mapping regional forest evapotranspiration and photosynthesis by coupling satellite data with ecosystem simulation. Ecology 70(4): 1090–101.

Running S, Thornton P, Nemani R, Glassy J. 2000. Global terrestrial gross and net primary productivity from the Earth observing system. In: Sala O, Jackson R, Mooney H, Eds. Methods in Ecosystem Science. Berlin Heidelberg. New York: Springer. p 44–57.

Safford LO. 1973. Fertilization increases diameter growth of birch-beech-maple trees in New Hampshire. USDA Forest Service Research Note NE-182. Darby (PA): USDA Forest Service.

Schimel D, Enting IG, Heimann M, Wigley TML, Raynaud D, Alves D, Seigenthaler U. 1995. CO_2 and the carbon cycle. In: Houghton JT, Meira Fihlo LG, Bruce J, Lee H, Chandler BA, Haites E, Harris N, Maskell K, Eds. Climate change 1994. Radiative Forcing of Climate Change and an Evaluation of the IPCC IS92 Emission Scenarios. Cambridge: Cambridge University Press.

Schimel DS, Braswell BH, McKeown R, Ojima DS, Parton WJ, Pulliam W. 1996. Climate and Nitrogen controls on the geography and timescales of terrestrial biogeochemical cycling. Global Biogeochem Cycles 10:677–92.

Schoettle AW. 1990. The interaction between leaf longevity, shoot growth and foliar biomass per shoot in *Pinus contorta* at two elevations. Tree Physiol 7:209–14.

Smith ML, Martin ME. 2001. A plot-based method for rapid estimation of forest canopy chemistry. Can J Forest Res 31:549–55.

Smith ML, Ollinger SV, Martin ME, Aber JD, Hallett RA, Goodale CL. 2002. Direct estimation of aboveground forest productivity through hyperspectral remote sensing of canopy nitrogen. Ecol Appl 12:1286–302.

Smith ML, Martin ME, Plourde L, Ollinger SV. 2003. Analysis of hyperspectral data for estimation of temperate forest canopy nitrogen concentration: comparison between an airborne (AVIRIS) and a spaceborne (Hyperion) Sensor. IEEE Trans Geosci Remote Sens 41(6):1332–7.

Townsend PA, Foster JR, Chastain RA. 2003. Imaigng spectroscopy and canopy nitrogen: application to forests of the central Applachian Mountains using Hyperion and AVIRIS. IEEE Trans Geosci Remote Sens 41(6):1347–54.

Tritton LM, Hornbeck VJW. 1981. Biomass equations for major tree species of the Northeast. USDA Forest Service General Technical Report NE-69 Broomall (PA): Northeastern Forest Experiment Station.

Tucker CJ, Sellers PJ. 1986. Satellite remote sensing of primary production. Int J Remote Sens 7:1395–416.

Turner DP, Cohen WB, Kennedy RA, Fassnacht KS, Briggs JM. 1999. Relationships between leaf area index and Landsat TM spectral vegetation indices across three temperate zone sites. Remote Sens Environ 70:52–68.

Turner MG, Gardner R, O'Neill R. 2001. Landscape Ecology in Theory and Practice. Berlin Heidelberg New York: Springer p, 401.

Ungar S, Pearlman J, Mendenhall J, Reuter D. 2003. Overview of Earth Observing-1 (EO-1) Mission. IEEE Trans Geosci Remote Sens 41(6):1149–59.

Vose JM, Allen HL. 1988. Leaf area, stemwood growth and nutritional relationships in loblolly pine. Forest Sci 34:547–63.

Wessman CA, Aber JD, Peterson DL, Melillo JM. 1988. Remote sensing of canopy chemistry and nitrogen cycling in temperate forest ecosystems. Nature 333:154–6.

Whittaker RH, Bormann FH, Likens GE, Siccama TG. 1974. The Hubbard Brook ecosystem study: forest biomass and production. Ecol Monogr 44(2):233–54.

Yin X. 1993. Variation in foliar nitrogen concentration by forest type and climatic gradients in North America. Can J Forest Res 23:1587–602.

Yoder BJ, Pettigrew-Crosby RE. 1995. Predicting nitrogen and chlorophyll content and concentrations from reflectance spectra (400–2,500 nm) at leaf and canopy scales. Remote Sens Environ 53(3):199–211.

Zagolski F, Pinel V, Romier J, Alcayde D, Gastellu-Etchegorry JP, Giordano G, Marty G, Mougin E. 1996. Forest canopy chemistry with high spectral resolution remote sensing. Int J Remote Sens 17:1107–28.